ELSEVIER

Contents lists available at ScienceDirect

Earth and Planetary Science Letters

www.elsevier.com/locate/epsl



Sediment and ocean crust both melt at subduction zones

Stephen J. Turner a,*, Charles H. Langmuir b

- ^a Department of Geosciences, University of Massachusetts, Amherst MA 01003, United States of America
- ^b Department of Earth and Planetary Sciences, Harvard University, Cambridge MA 02138, United States of America



ARTICLE INFO

Article history:
Received 14 June 2021
Received in revised form 13 January 2022
Accepted 7 February 2022
Available online xxxx
Editor: R. Dasgupta

Keywords: slab melting subduction arc geochemistry

ABSTRACT

Hydrous arc magmas are produced when water-bearing materials from subducted oceanic plates are transported to the mantle beneath volcanic arcs, though the mechanism of mass transport remains debated. The geochemical characteristics of the slab component have important implications for the thermal structures of down-going plates and the fluxes of elements into the deep mantle. If slab temperatures are low, then elemental fluxes from the slab will be carried in a dilute fluid. If temperatures are high, the slab may melt instead. While a long-standing paradigm for arc volcanism has been that sediments melt and ocean crust dehydrates, a growing body of evidence from arc geochemistry and experimental petrology suggests both sediment and ocean crust melt. The low solubility of many elements in aqueous fluids prevents them from making a substantial contribution to arc mass-balance. Constraints from Sr concentrations and 87Sr/86Sr ratios require a large flux of Sr from the ocean crust, which is only possible if the crust melts. H₂O/Sr ratios of arc volcanics are also inconsistent with slab fluids. These conclusions are supported by thermo-mechanical models indicating that slab temperatures exceed the hydrous solidus for both ocean crust and sediments. Examination of experimental data shows a likely strong effect of oxygen fugacity on residual phases during slab melting. Arc data are best explained if the ocean crust melts beneath all arcs under oxidizing conditions somewhere between FMQ and NNO+2. Experimental constraints on sediments also require melting and that sediment melt compositions depend on bulk composition as well as temperature. If these experiments serve as analogs to sediment melting beneath arcs, then sediment bulk compositions are a necessary input for any rare earth element-based slab thermometer. We present compositions for ocean crust partial melts and partition coefficients for sediment melting based on existing experiments, physical models, and arc data, that can be used in geochemical models of arc volcanism.

© 2022 Elsevier B.V. All rights reserved.

1. Introduction

Arc volcanoes are the product of water recycling from the subducting plate into the mantle above, though exactly how water and other slab-derived components are delivered to the mantle source is poorly constrained. One uncertainty is whether the hydrous phase is a fluid, melt, or both. Within the pressure interval anticipated for the region of mantle melting beneath arcs the water-bearing phase will be an aqueous fluid with >85 wt.% H₂O if temperatures are low, or a hydrous melt with <35 wt.% H₂O if temperatures are higher. The transition between these phases occurs across a narrow temperature interval (Manning, 2004; Kessel et al., 2005; Hermann and Spandler, 2008). The fluid and melt phases have very different compositions and transport properties. If the liquid phase is an aqueous fluid, a colder slab thermal gra-

dient can be inferred, and a substantial quantity of incompatible elements will be subducted beyond the arc into the deep mantle. Hydrous melts imply a hotter slab, and a smaller elemental return flux to the mantle. The relative importance of fluids and melts from the slab thus has far-reaching implications for the thermal structure of the subducting plate, the source of elements to the arc and their medium of transport, the fate and composition of recycled plates, and the creation of continental crust and mantle heterogeneity.

At higher pressures water may also be transported as a supercritical fluid with continuously varying $\rm H_2O$ concentrations. Kessel et al. (2005) and Ni et al. (2017), however, provide evidence that the second critical endpoint for the slab occurs at >150 km depth, which is well beyond the 110 km slab depth that is typical beneath arcs. In view of the thermal models discussed below, most slab dehydration reactions and melting likely occur at much shallower depths than where a super-critical fluid would be stable.

^{*} Corresponding author.

E-mail address: stephenjudsonturner@gmail.com (S.J. Turner).

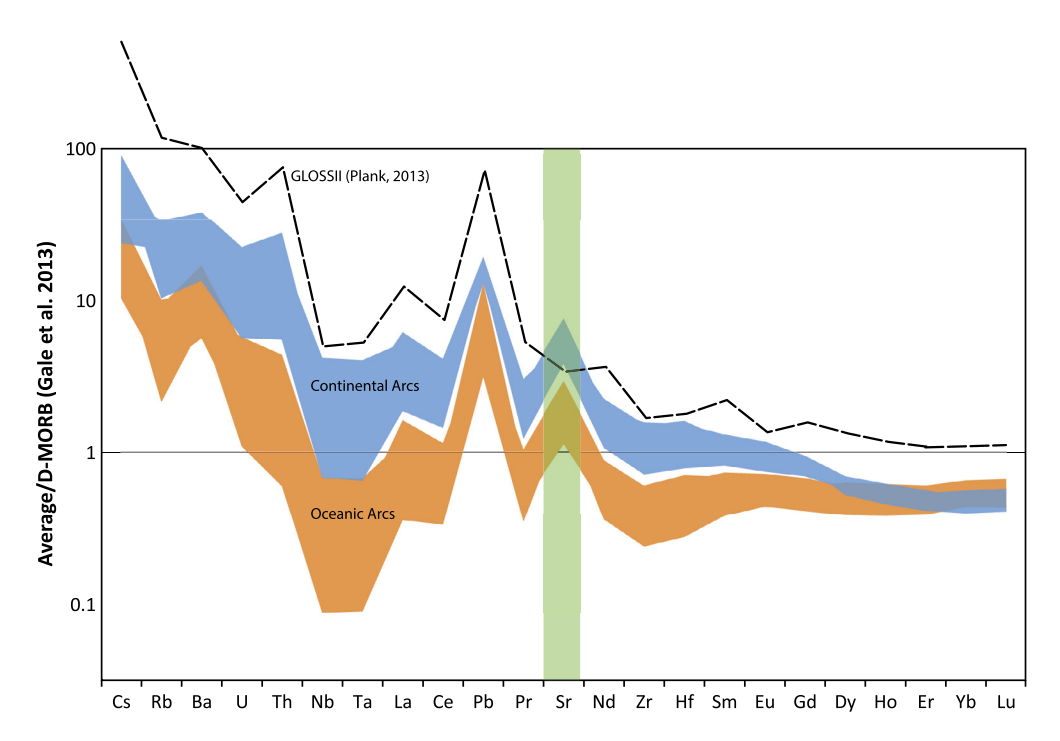


Fig. 1. Spider diagram depicting the compositional ranges of high-Mg# samples from oceanic arcs with thin crust and continental arcs with thick crust normalized to DMORB from Gale et al. (2013). The GLOSSII weighted average subducting sediment composition of Plank (2013) is plotted for comparison. Note that positive Sr anomalies are ubiquitous in arc-front volcanics but absent in most sediment. The arc data used to create these fields were compiled by Turner and Langmuir (2022), who discuss multiple lines of evidence that the data are generally representative of parental compositions from continental and oceanic arc-front stratovolcanoes. Samples from small free-standing cones and volcanic edifices away from the arc front can have more exotic compositions but are not representative of the main volume of the arc. Volcanoes from regions with additional tectonic complexity, such as intra-arc rifting or subducting ridges, fracture zones, and oceanic plateaus are also excluded. For an extended discussion of this data, see Turner and Langmuir (2022).

Trace element and isotopic studies of arc rocks have revealed distinct geochemical signatures that require slab contributions from both subducting sediment and altered ocean crust (AOC) (e.g., Ellam and Hawkesworth, 1988; Miller et al., 1994; Elliott et al., 1997; Class et al., 2000). Because slab dehydration proceeds continuously (Schmidt and Poli, 1998), some portion of the slab must dehydrate without melting. The AOC component could therefore be a fluid sourced from deeper within the slab, and the sediment component a melt from the hotter slab surface. This possibility is supported by the finding that the AOC component is enriched in elements such as Rb, Ba, U, and Pb (Miller et al., 1994; Elliott et al., 1997), that are also more soluble in experimental fluids (Brenan et al., 1995). The distinction between these "fluid-mobile" elements and "sediment-melt" elements such as the REE and Th has since become entrenched as an important aspect of models of arc magma petrogenesis (e.g., Elliott, 2003 and references therein).

While 'AOC fluids' are a hallmark of many models, Kelemen et al. (2003a, 2003b) argued that partial melts of both ocean crust and sediment might be more consistent with arc data. Recent experimental studies support this view, demonstrating that elemental fractionations usually attributed to fluids may also arise from AOC melting (e.g., Klimm et al., 2008). Melting experiments on natural ocean basalts have stabilized either apatite (Sisson and Kelemen, 2018) or epidote (Carter et al., 2015), which retain light rare earth elements (LREEs) and Th, leading to high ratios such as U/Th and Ba/Th that have previously been attributed to fluids. These experimental advances have led several recent studies to propose that AOC melting might occur even when the subducting slabs are colder. Turner and Langmuir (2015) and Turner et al. (2016), for example, suggested that global variations in trace element concentrations require melting of both sediments and oceanic crust. Freymuth et al. (2016) used thorium isotopic evidence in Izu (often considered one of the world's coldest slabs) to argue for AOC melting, and Yogodzinski et al. (2017) proposed that AOC melts dominate the Sr budget for lavas throughout the Aleutian arc.

Though various studies have proposed ocean crust melting beneath arcs, a more common view is that AOC only melts in a small set of unique tectonic settings to produce adakites (Defant and Drummond, 1990), which are distinguished by extreme enrichment in Sr and depletion in the heavy rare earth elements (HREE). More typical arc magmas are also enriched in Sr and depleted in the HREE relative to MORB, however (Fig. 1), so the adakite signature could simply be the end member of a process that contributes to all arcs (Yogodzinski et al., 2017). Indeed, the ubiquitous positive Sr anomaly in arcs is one of the central observations that must be accounted for by successful models of arc volcanism.

An aqueous fluid phase from altered ocean crust remains central to many studies, however, and the term "fluid-mobile elements" has become part of the petrogenetic lexicon. It has been suggested that many oceanic arcs lack a melt component entirely (Schmidt and Jagoutz, 2017), though a more common view is that sediments melt in most arcs, while the ocean crust often remains below the solidus, leading to dehydration without melting. This general model has been applied to many arcs (e.g., Miller et al., 1994; Elliott et al., 1997; Class et al., 2000; Singer et al., 2007; Duggen et al., 2007; Labanieh et al., 2012; Klaver et al., 2020), and has also been invoked to account for mantle heterogeneity observed at ocean ridges (Dixon et al., 2017).

These diverse interpretations show that despite its centrality to our understanding of arc volcanism, the nature of the slab flux remains contentious. Here, we re-evaluate the relative importance of melts and fluids from the slab using four lines of evidence – thermal models of subducting slabs, mass-balance relating subducting fluxes to arc outputs, experimental studies that constrain melt and fluid compositions, and arc lava geochemistry. Together, these show that melting of ocean crust as well as sediment is most plausible.

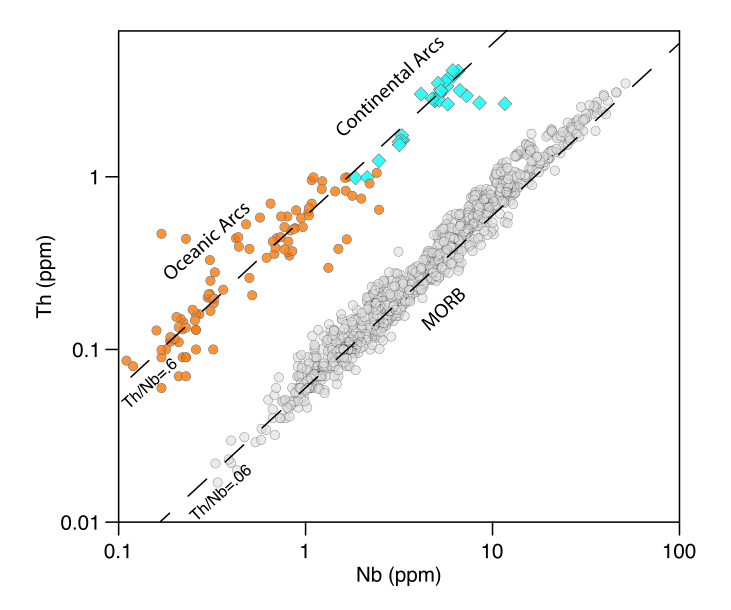


Fig. 2. Comparison of Th and Nb abundances in high-Mg# samples from arc-front stratovolcanoes (as compiled by Turner and Langmuir, 2022) and MORB (Gale et al., 2013). At any given Nb concentration, arcs have about an order of magnitude greater Th. This requires Th mobilization from sediment, which in turn requires sediment melting.

2. Evidence for melting of both sediment and AOC

Diverse lines of evidence converge to show that both sediments and AOC usually melt at convergent margins, even at the "coldest" subduction zones.

2.1. Evidence that sediments melt

Arcs are enriched in Th relative to the REE (Fig. 1), and Th systematics of volcanic arcs provide strong evidence for melting of subducting sediment. Because sediments dominate the budget of Th in subducting plates (cf., Gale et al., 2013; Plank, 2013), and arc Th abundances correlate with the amount of Th being subducted (Plank and Langmuir, 1993; Plank, 2005), the Th excesses in arcs are most likely derived from subducted sediment. Experiments have consistently found Th to be insoluble during slab dehydration beneath arcs (Brenan et al., 1995; Johnson and Plank, 2000; Kessel et al., 2005; Spandler et al., 2007; Rustioni et al., 2019). Sediment fluids would thus fractionate certain element ratios such as Rb/Th in ways that are not seen in arcs, requiring that transport from sediments must instead occur via a higher temperature hydrous melt (Johnson and Plank, 2000).

This conclusion is reinforced by thorium-niobium systematics of arcs (Fig. 2). Away from subduction zones, Th and Nb behave similarly, leading to remarkably constant Th/Nb ratios (Fig. 2). Arcfront stratovolcanoes have much higher Th/Nb ratios than MORB, requiring efficient transfer of Th from the subducting plate. Many arcs have even higher Th/Nb than corresponding bulk sediments, which is consistent with the presence of residual rutile during sediment melting near the slab surface (e.g., Elliott, 2003; Skora and Blundy, 2010). This is also one of several reasons (see Turner and Langmuir, 2022, for an extended discussion) that bulk sediment transport to the wedge, such as in a diapir, is implausible. Th-Nb systematics are thus also most consistent with sediment melting.

The geochemical evidence for sediment melting was at odds with some early thermal models of subduction zones (Poli and Schmidt, 2002), though models incorporating temperature-dependent viscosity have long supported conditions suitable for melting on the slab surface (Furukawa, 1993; Van Keken et al., 2002; Kele-

men et al., 2003c). Sediment melting is thus supported by experimental data, arc geochemistry, and geophysical modeling.

2.2. Evidence from thermal models

The water-saturated solidus of altered ocean crust is very similar to sediment (Spandler and Pirard, 2013), so if the sediment melts, and the sediment layer is thin, then ocean crust melting is also likely. The thickness of the subducting sediment layers measured on the seafloor or observed in the shallow portions of the "subduction channel" above the slab are inevitably thicker than the sediment layer at depth, because of the later expulsion of pore fluids and the transition to eclogite. For example, the median \sim 400 m seafloor sediment thickness in the compilation of Plank (2013) should be compressed to \sim 150 m after conversion to eclogite based on observed porosity and density. Furthermore, sediment melt fractions can exceed 30% under water saturated conditions (Schmidt et al., 2004). Therefore, only a thin veneer of sediment likely remains present beneath the arc, resulting in similar temperature-pressure conditions for sediment and AOC, supporting the idea that both AOC and sediment will melt.

In addition, thermo-mechanical models that match heat flow constraints and incorporate realistic slab profiles (e.g., Wada and Wang, 2009; van Keken et al., 2018), have converged on hotter overall slab temperature profiles, with the water-saturated solidus penetrating well into the ocean crust in even the coldest subducting slabs (Fig. 3a). On Fig. 3c-e, the phase boundaries from experimental studies and thermodynamic models (Fig. 3a-b) have been projected onto the modeled slab temperature fields of van Keken et al. (2018). It is apparent from these projections that the upper layers of the slab reach temperatures that exceed the hydrous solidus just as lawsonite dehydration releases water from the underlying layers. These models thus support water-saturated melting of at least the top 1 km of the slab, even when convergence rates are high and subducting plates are old. Very young slabs will have hotter internal temperatures and may be unable to retain lawsonite to sub-arc depths, in which case zoisite breakdown could replace lawsonite as the source of water (Fig. 3a, Schmidt and Poli, 1998). The petrological tools commonly used to model slab dehydration do not yet reproduce experimental results regarding zoisite stability (Wei and Duan, 2019), however, limiting the utility of this common modeling approach for hotter slabs. Overall, these results show that AOC melting is plausible and consistent with the thermal models, even for the coldest slabs.

Serpentinite within the lithospheric mantle of the subducting plate (the slab-mantle) serves as another potential fluid source. The slab-mantle temperatures in the Tongan slab model never exceed the stability limits of antigorite, however, while in Izu, antigorite breakdown is predicted about 50 km behind the arc front. Antigorite breakdown occurs somewhat closer to the arc front in the Marianas. None of these models have slab-mantle temperatures exceeding the chlorite stability field near the arc front, however (Fig. 3b). Antigorite breakdown fluids may therefore be consumed by the production of chlorite, with no net fluid loss from the lithospheric mantle, depending on the initial hydration level and the spatial distribution of hydrous phases in the slab-mantle (Wada et al., 2012). It is also possible that any fluids released from the slab-mantle would be consumed by hydration reactions in the overlying gabbro (Wada et al., 2012), which has a large potential water capacity prior to lawsonite breakdown (Schmidt and Poli, 1998). While lawsonite is likely to break down in the upper crust where temperatures are higher, the lowermost crusts of all but the very hottest slabs are predicted to retain lawsonite well beyond the arc front (Fig. 3a). It is therefore plausible that any water initially present in the slab-mantle is usually subducted beyond the arc. This conclusion is consistent with the synthesis of Bekaert et

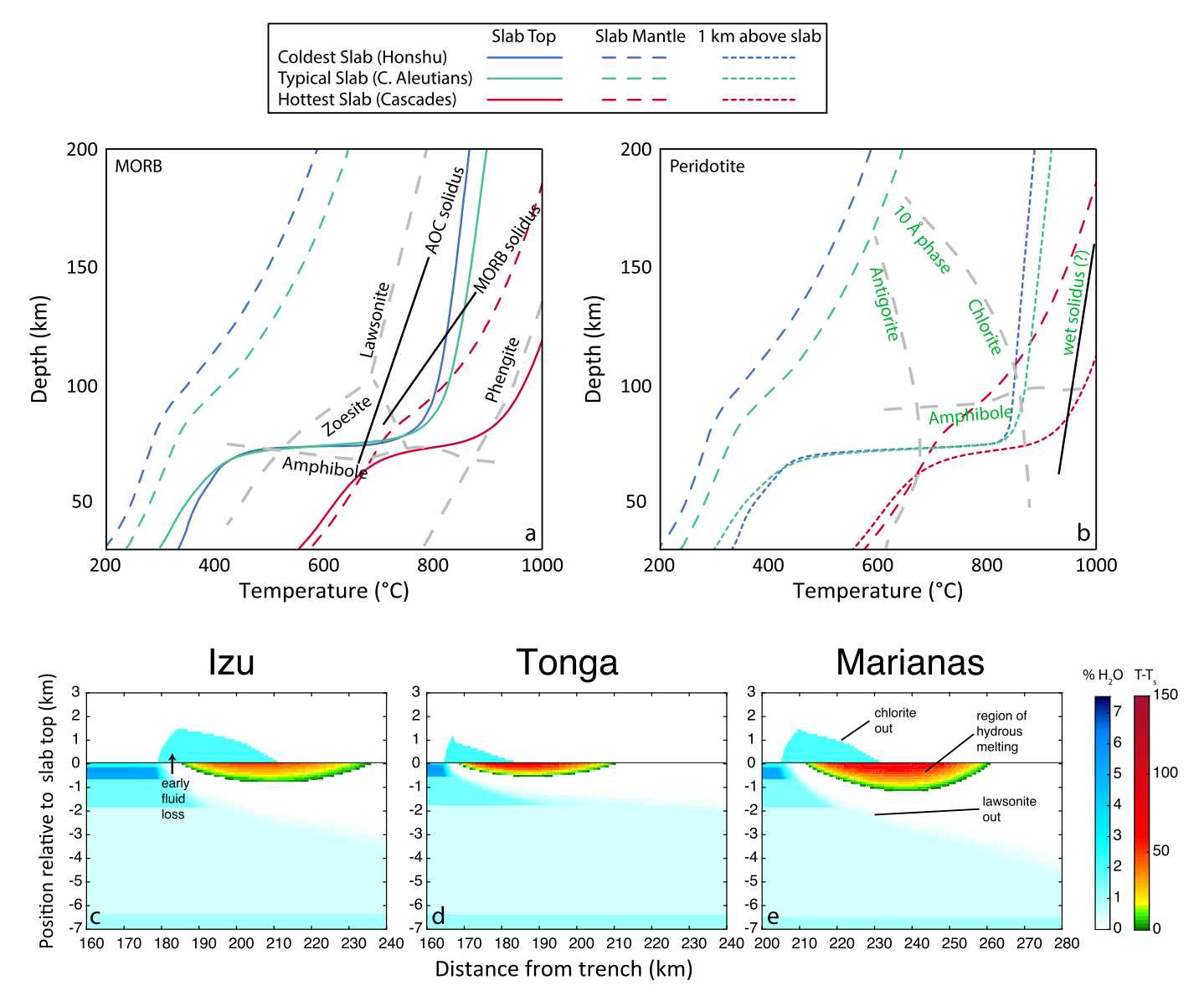


Fig. 3. (a-b) Examples of slab thermal profiles at various slab depths as compared to stability fields of important hydrous minerals. Slab thermal profiles are from the "farb2" model set of van Keken et al. (2018), which provides the best match to fore-arc heat flow data (see Fig. 10b of van Keken et al., 2018). Phase boundaries are after Schmidt and Poli (1998) and Fumagalli and Poli (2005). The water-saturated solidus for altered ocean crust is after Spandler and Pirard (2013) and the 'MORB' water-saturated solidus is after Sisson and Kelemen (2018). The slab profiles in panels a-b in were selected to depict the global range of slab temperatures. (c-e) Horizontal projections of the subducting slab and immediately overlying mantle relative to its distance from the "farb2" models (P-T grids were provided by van Keken, personal communication). The slab models in panels c-e were selected in order to demonstrate the plausibility of slab melting in various convergent margins that have older subducting plates. In regions where the slab temperature exceeds the solidus, a color gradient is plotted to depict T-Ts, which is the difference between T and the water-saturated AOC solidus T (Ts) at the relevant pressure. These results support the plausibility of melting of subducted ocean crust. Water lost beyond the depth of coupling but prior to the onset of slab melting is transported above the slab where it is held in chlorite (chlorite field after Grove et al., 2012), which is assumed to carry a maximum of 12% H₂O. In each of these cases, the interval of chlorite dehydration corresponds with the interval of melting of the slab below. (For interpretation of the colors in the figure(s), the reader is referred to the web version of this article.)

al. (2021), who found that H_2O mass-balance across subduction zones does not require any input of fluids from the lithospheric mantle.

Thermal models and phase equilibria are thus consistent with ubiquitous melting of AOC.

2.3. Sr mass-balance constraints

The Sr systematics of arcs place further constraints on the importance of AOC melts vs. AOC fluids. Sr is advantageous because (1) all arc-front stratovolcano parental magmas have prominent positive Sr anomalies, while non-carbonate sediments lack such anomalies (Fig. 1), and (2) arc parental magmas have low ⁸⁷Sr/⁸⁶Sr

(generally .703 to .7045) compared to sediments (0.7124 in average sediment; Plank, 2014) which limits the Sr that can be derived from sediment. In a few arc segments higher ⁸⁷Sr/⁸⁶Sr basalts have erupted, but these rocks have been linked to either upper crustal assimilation or unusually thick sediment thickness on the subducting plate (e.g., Davidson and Harmon, 1989; Bezard et al., 2014; Handley et al., 2014; Aiuppa et al., 2017). Based on these constraints, it has long been established that most of the excess Sr in typical arc parental magmas must be derived from the subducting ocean crust (e.g., Kelemen et al., 2003a; Gómez-Tuena et al., 2007).

To quantify the ocean crust Sr contribution to an arc, the contributions from the ambient mantle (i.e., the mantle composition prior to slab addition) and sediment must be subtracted from the

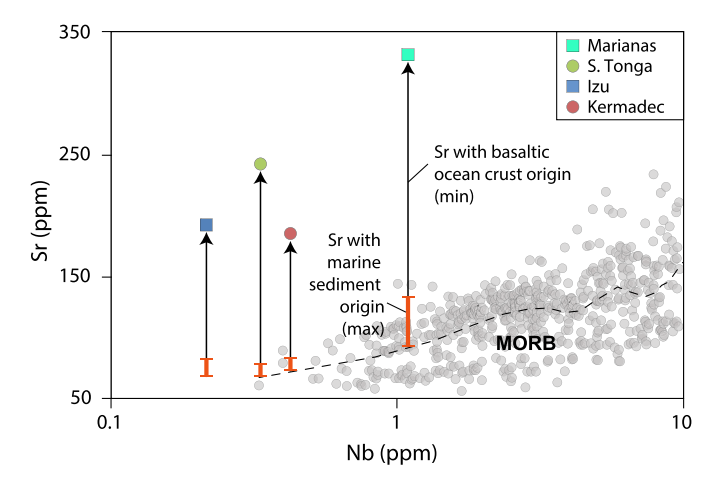


Fig. 4. Illustration of how to quantify the excess Sr in various arcs. The Nb-Sr relationships of MORB show how Sr content varies with Nb content due to variations in ambient mantle enrichment and extents of melting. The dashed line is a running average through the MORB data. Compared to MORB, arcs are offset to higher Sr at a given Nb, which must result from the slab flux. Average Sr contents of high-Mg# samples without negative or positive europium anomalies are shown for each arc (Turner and Langmuir, 2022). Since Sr in sediments is low in abundance but very high in ⁸⁷Sr/⁸⁶Sr, most of the excess Sr must be derived from the subducted basaltic crust (see discussion in text). The arcs in this figure were selected as typical oceanic subduction zones associated with colder slabs, due to the rapid descent of old oceanic plates, that also have back-arc basin basalt data that can be used to constrain ⁸⁷Sr/⁸⁶Sr of the ambient mantle (see online supplement). The Sr excesses seen in these arcs, coupled with experimental constraints on Sr partitioning (Fig. 5), show that the ocean crust must melt even when old plates subduct at high velocity.

total arc Sr. Fig. 4 compares the average Sr and Nb concentrations of representative high-Mg# oceanic arc-front stratovolcano samples to MORB data that have been filtered to remove samples strongly affected by plagioclase fractionation (see figure caption). The MORB data show how much Sr is derived from the upper mantle for a given Nb content irrespective of differences in extents of melting or mantle heterogeneity. The Nb in arc magmas is largely derived from the ambient mantle. The vertical offsets in Sr abundances between arcs and MORB reflect Sr that was added from the slab. If some Nb were also slab-derived, the arc data points would need to be translated to lower Nb, requiring even more Sr from the slab. This method makes it possible to determine the minimum amount of Sr that is slab-derived without arbitrarily assuming ambient mantle Sr concentrations or extents of mantle melting.

The ⁸⁷Sr/⁸⁶Sr of the ambient mantle can be estimated from back-arc basin basalts that have negligible subduction-related trace element anomalies (see also, Turner and Langmuir, 2022). Typical ocean crust alteration has a minor impact on Sr abundances but raises the average 87 Sr/86 Sr of the upper 500 m of ocean crust by about 0.0017 (Staudigel et al., 1995), with only minor increases in ⁸⁷Sr/⁸⁶Sr in the deeper layers of the slab (Bach et al., 2003). Given that at least the upper 1.5 km of the slab should dehydrate near the arc front (Fig. 3c-e, van Keken et al., 2018), the typical composition of Sr extracted from dehydrating ocean crust in these arcs should have ${}^{87}\text{Sr}/{}^{86}\text{Sr}$ of \sim 0.7032, between average Pacific MORB (${}^{87}\text{Sr}/{}^{86}\text{Sr}$ =0.70257, Gale et al., 2013) and an upper slab layer with 87 Sr/ 86 Sr \sim 0.7043. This estimate based on drill core samples is consistent with the compositions of samples dredged from large normal faults offshore Izu by Durkin et al. (2020). Because average subducting sediment ⁸⁷Sr/⁸⁶Sr compositions (Plank, 2013) are all much higher (mostly >0.709), isotope mass-balance for most arcs limits sediment-derived Sr to <13% (or 11% if AOC ⁸⁷Sr/⁸⁶Sr=0.7033) of the excess Sr (Fig. 4, Table S1).

About 150 ppm or more of the Sr in these arcs must therefore be derived from the subducted ocean crust, which requires efficient extraction. While the ocean crust is 6-7 km thick, only the top 3 km (top 1.5 km for Tonga, where convergence is very fast)

of the crust will dehydrate or melt in these arcs (Fig. 3c-e, van Keken et al., 2018) and hence be capable of delivering Sr to the wedge. Given convergence rates of 45 to 65 km/Ma (\sim 165 km/Ma for Tonga), 135 to 195 km³ of subducted ocean crust will thus dehydrate per Ma for each kilometer of arc. Calculations of the Sr flux into the upper plate depend on arc magma production rates. For oceanic arcs, estimates of magma production rates (Dimalanta et al., 2002; Jicha and Jagoutz, 2015) range from 55-89 km³ per km of arc per Ma (or much higher if arc erosion or delamination rates have been significant). To supply 150 ppm Sr to 75 km³ of arc crust from 165 km³ of subducting crust (with 128 ppm Sr, Gale et al., 2013), at least half of the Sr must be extracted from the portion of the subducting crust that dehydrates, implying very substantial Sr mobilization and transport.

For such efficient extraction to occur, Sr must strongly partition into the liquid phase. If the liquid phase is a fluid with >85% $\rm H_2O$, then the relative mass of that phase is constrained by the total available water. The total water content of subducted altered ocean crust subducted beyond the forearc is <2 wt.% (Schmidt and Poli, 1998, Fig. 3c-e), so a small total volume of fluid would need to extract half the Sr. Simple mass balance shows that if the total fluid fraction is \sim 1%, then extracting half the Sr is only possible if the solid/fluid partition coefficient (DSreclogite/fluid) is \sim 0.02. A partial melt of the crust, on the other hand, is not as constrained by mass. If the same mass of water were carried within a hydrous melt with <10% $\rm H_2O$, for example, melt fractions in the slab could reach 10-20%, and mass balance would be met given DSreclogite/melt from 0.1 to 0.2. These requirements can then be compared to experimental constraints on solid/fluid and solid/melt partitioning.

Recent experiments (Rustioni et al., 2019) show that Sr does not partition strongly into an aqueous fluid unless chlorine contents are very high. DSr^{eclogite}/fluid values range from ~0.5 at moderate to low salinity to under 0.1 at very high salinity (Fig. 5a). This general increase in incompatible element mobility at high fluid salinity led Castillo (2021) to suggest that the slab component might be a Cl-rich fluid. Independent constraints on the possible salinity of slab fluids are available from the H₂O/Cl ratios of arcs. Magmatic Cl abundances are not retained in erupted lavas but are reliably preserved in olivine-hosted melt inclusions with mafic compositions. For the Marianas arc, ample melt-inclusion data (e.g., Brounce et al., 2014) allow estimation of the primary magma compositions, which contain \sim 0.05 wt.% Cl (see Figure S1) and \sim 4 wt.% H₂O (Plank et al., 2013), consistent with about 1 wt.% Cl in a pure fluid component. This estimate agrees well with independent constraints from Li and Hermann (2015). Based on the Rustioni et al. (2019) experiments (Fig. 5), this would suggest DSreclogite/fluid of \sim 0.2, which is an order of magnitude too high to meet the Sr mass balance requirements. This value is also in agreement with several other eclogite-fluid and fluid-melt partitioning experiments that have utilized a wide range of sophisticated experimental techniques (Brenan et al., 1995; Keppler, 1996; Stalder et al., 1998; Kessel et al., 2005; Spandler et al., 2007; Borchert et al., 2010; Kawamoto et al., 2014). If lawsonite, epidote, phengite, or apatite were present, as is likely for AOC (Carter et al., 2015; Sisson and Kelemen, 2018), DSreclogite/fluid would be higher and Sr even less mobile (Spandler and Pirard, 2013). Fluids produced by dehydration reactions in the subducting crust are thus unable to transport enough Sr from the AOC to account for the arc Sr budget.

An alternative approach makes use of Cl/Sr ratios. Given 128 ppm Sr in the ocean crust (Gale et al., 2013), the Cl and Sr aqueous fluid partitioning values from the Rustioni et al. (2019) experiments with >2% Cl would produce fluids with Cl/Sr>16, while arc melt inclusions have Cl/Sr of \sim 4.5 or lower (Fig. 5b). Cl contents that are high enough to mobilize Sr would thus inevitably produce fluids and associated arc magmas with Cl/Sr contents that are far

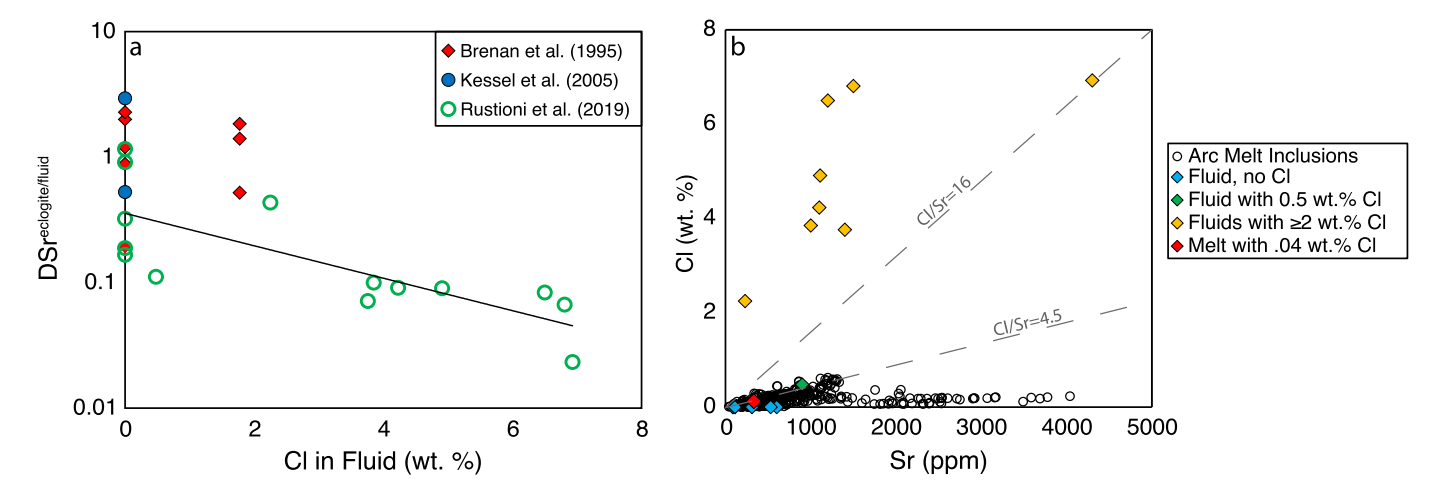


Fig. 5. (a) Experimental Declogite/fluid values from Brenan et al. (1995), Kessel et al. (2005), and Rustioni et al. (2019) as a function of CI content in the fluid. High CI fluids result in lower D values and greater Sr mobility (b) CI vs Sr abundances of the Rustioni et al. (2019) experiments are compared to olivine-hosted melt inclusions from arcs with greater than 6 wt.% MgO (via GEOROC). Fluid Sr abundances are calculated using D values reported by Rustioni et al. (2019) and average MORB Sr abundances (Gale et al., 2013). Because CI and Sr are both incompatible elements, CI/Sr in melts will not be strongly fractionated during melting. For a successful 'slab fluid' model, arc samples must therefore fall along mixing lines between fluid compositions and the ambient mantle (essentially at the origin of this plot). The high CI experiments of Rustioni et al. (2019) plot far above any possible mixing line, demonstrating that fluids with such high CI abundances are not viable. If the actual slab component were a fluid, it must therefore have a lower CI/Sr ratio than most of the experiments of Rustioni et al. (2019), with an upper limit of ~1 wt.% CI. At these lower CI concentrations, the relationship between CI and DSr (panel a) indicates an average SrDeclogite/fluid of ~0.2. Also shown on (b) is a melt composition from a natural MORB sample (Sisson and Kelemen, 2018), which has a CI/Sr value that matches most arc data.

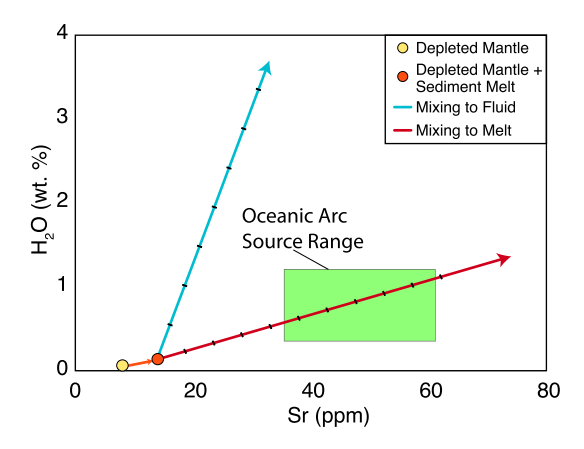


Fig. 6. The requirement for slab melts can be visualized on a plot of mantle source contents of Sr vs H_2O . The possible compositional range of the oceanic arc mantle sources (see text) has been calculated for the arcs shown on Fig. 5 using partition coefficients from Workman and Hart (2005) (assuming $DC=DH_2O$). The addition of sediment melt (which is constrained by isotopic mass balance) to the mantle source shifts the depleted mantle composition only slightly towards the required oceanic arc mantle source range. From this point, adding aqueous fluids to the mantle results in a trajectory with H_2O/Sr that is far higher than arc mantle source range. The addition of AOC melts, in contrast, reproduces the required source compositions. Currently available experimental evidence thus appears to require melting of ocean crust as well as sediment, even in arcs like Tonga where the oldest plates are descending the most rapidly. Each tick represents a 1% addition of slab melt or fluid to the mantle wedge.

higher than what is observed. Hydrous fluids, no matter what their Cl content, cannot meet the Sr constraints.

Fluids interacting with the subducting ocean crust would also lack the appropriate ratios of water to Sr, regardless of water:rock ratios. Average arc Sr abundances (Table S1) can be used to calculate the plausible compositional range of Sr and H₂O in the oceanic arc mantle sources, assuming 2-6% primary H₂O and 15-20% mantle melting. A small amount of Sr can be added by a sediment melt (as in Fig. 4). Fig. 6 shows that adding a fluid with 90 wt.% H₂O and 600 ppm Sr results in a mixing trajectory with H₂O/Sr greatly exceeding the plausible mantle range. Therefore, even if the fluids from the dehydrating ocean crust were augmented by water from dehydrating slab-mantle antigorite that somehow permeated

the crust, equilibrated with lower crustal rocks, and then became remobilized out of the crust and into the mantle wedge, the resultant fluid composition would be inconsistent with the compositions of arcs, because their H₂O/Sr ratios would be too high.

This source calculation is a simplified version of the approach used by Stolper and Newman (1994) to determine the composition of a single hypothetical slab component transferred to the Marianas mantle source. Stolper and Newman's proposed slab component was a hydrous fluid with *several thousand* ppm Sr. Such high Sr contents clearly violate constraints from the fluid partitioning experiments that have since become available.

Melts, by contrast, can readily transport sufficient Sr due to a slightly lower D value during melting and because melting produces a much larger total liquid fraction with lower $\rm H_2O$ contents. Stolper and Newman (1994) required very high Sr contents in their slab component because their $\rm H_2O$ concentration was arbitrarily set to fluid-like values. If the water fraction were lowered to melt-like values instead, then the required Sr contents would also be lower, and consistent with experiments that show DSreclogite/melt $\sim\!0.1$ (e.g., Kessel et al., 2005; Sisson and Kelemen, 2018). Mass balance would then be satisfied by 10% fractional melting of the slab, which would extract 65% of the bulk Sr from the portion that melted. Adding a melt with $\sim\!10$ wt.% $\rm H_2O$ also accounts well for the arc compositions on Fig. 6. The AOC "hydrous component" is thus most consistent with a melt.

These various approaches to the arc Sr budget all arrive at the same conclusion. Elemental and isotopic mass-balance require a large flux of Sr from the subducted ocean crust, which is difficult to produce with a fluid. Cl/Sr ratios are inconsistent with a mode of transport by high Cl fluids. Experiments indicate that AOC fluids will have higher H₂O/Sr ratios than what is required to explain arc volcanics. Experiments and arc data are thus most consistent with melting of mafic ocean crust, in addition to melting of sediment.

3. Calculation of melt compositions from altered ocean crust and sediment

If both sediments and AOC melt, then quantitative models of arc volcanism require calculations of slab melt compositions that are consistent with both experiments and natural arc lavas.

3.1. Constraints on AOC melt compositions

One of the arguments for fluid transfer from the slab to the wedge is the enrichment of "fluid mobile elements" such as Ba, Pb, and Sr, relative to the REEs, Nb, and Ta. Recent experimental data, however, have found that melts of altered oceanic crust also have these characteristics (Klimm et al., 2008; Carter et al., 2015; Sisson and Kelemen, 2018). The ²³⁸U-excess typical of many volcanic arcs is commonly invoked as additional evidence for a fluid component (Elliott, 2003), but can also result from melting (Avanzinelli et al., 2012; Carter et al., 2015). While these results suggest slab melts alone can produce the array of elemental anomalies that characterize arcs, there are also important differences among the experiments. Here, we show that compositions of AOC melts can be further constrained by relating forward models based on experimental results to the compositions of arc volcanics.

Kessel et al. (2005) was the first experimental study to measure elemental partitioning among a large suite of trace elements during melting of a MORB-like bulk composition. While the bulk partition coefficients reported by Kessel et al. (2005) remain widely used, their utility is limited by (1) the lack of K₂O, which controls the position of the solidus and the total melt fraction (Schmidt et al., 2004), and (2) that they were calculated between melts and clinopyroxene+garnet, while it was later discovered that the budgets of many trace elements in these experiments were dominated by accessory phases that were not initially identified (Klimm et al., 2008). As a result, the bulk partition coefficients reported by Kessel et al. (2005) for the LREE, Th, and U violate mass balance and do not accurately reflect the actual eclogite-liquid partitioning that was present in the experiments.

Experiments that have accounted for the presence of accessory phases have produced diverse results, which may be due to differences in the doping levels, oxygen fugacity, and K_2O contents. Klimm et al. (2008) used a similar bulk composition to Kessel et al. (2005), but with added K_2O and oxygen fugacity buffered near NNO. They showed that under these conditions accessory allanite limited the melt mobility of the LREE, Th, and U (Fig. 7a). Because the trace element doping levels of the experiments were high, however, the stability of allanite was enhanced relative to natural AOC.

Carter et al. (2015) measured partitioning in melts of natural, undoped MORB and AOC samples, but under highly oxidized experimental conditions (\sim NNO+2 or greater, depending on H₂O loss). These experiments produced residual epidote–clinozoisite rather than allanite. While LREEs generally partition more strongly into allanite than other epidote–group minerals (Frei et al., 2003), the mobilities of LREE in the Carter et al. (2015) AOC-melting experiments were equal to or lower than Klimm et al. (2008) (Fig. 7a).

Sisson and Kelemen (2018) expanded on the experimental work of Liu et al. (1996), who melted natural K_2O -bearing MORB buffered at more reducing conditions (QFM). They identified residual apatite rather than epidote or allanite and found substantially greater REE mobility (Fig. 7a). Luginbühl (2015) conducted melting experiments at NNO and more moderate doping levels but with very high (5 wt.%) K_2O , which produced high melt fractions, early exhaustion of epidote, and melts with intermediate REE mobility compared to other studies (Fig. 7a).

These results suggest that in addition to doping levels, oxygen fugacity plays an important role in trace element mobility, because epidote contains Fe³⁺ and its stability is enhanced under oxidizing conditions. The relatively reduced experiments of Sisson and Kelemen (2018) probably destabilized epidote, while the oxidizing conditions of Carter et al. (2015) stabilized it, with consequences for LREE mobility (Sisson, personal communication).

Volcanic arc compositions provide additional context for these experiments. Fluxes of Sr from the slab must be large relative to Ce and Nd (Fig. 1). The magnitude of the Sr enrichment can be quantified as $Sr/Sr^*=Sr_N/(Ce_N^*Nd_N)^{1/2}$ (normalized to C1 chondrite values of Sun and McDonough, 1989). Arc magmas, once filtered to remove samples with obvious plagioclase fractionation or accumulation, generally have Sr/Sr* between 2 and 4 (Sisson and Kelemen, 2018). Fig. 7b demonstrates the effects of mixing different slab melts into the depleted mantle. The Sr, Ce, and Nd abundances in the melts are calculated based on the melt partitioning in each experiment, renormalized to a bulk composition of average MORB (Gale et al., 2013). This diagram shows that mixing between the mantle wedge and the oxidized experimental melts of Carter et al. (2015) (or the highly doped experiments of Klimm et al., 2008), in which the stability of REE-bearing phases is enhanced, produces an excessively high Sr/Sr* (Fig. 7b). Mixing to the more reduced Sisson and Kelemen (2018) experimental melts, on the other hand, produces Sr/Sr* that is too low.

Intermediate REE mobility is also indicated by the nominal to negative Zr-Hf anomalies of arc volcanics $[Zr/Zr^*=Zr_N/(Nd_N^*Sm_N)^{1/2}]$. Zr and Hf are less likely to be affected by oxygen fugacity, and bulk Zr concentrations are close to natural abundances even in doped experiments, providing a useful basis of comparison to the REE. Most arc data have Zr/Zr^* between 0.4 and 1, whereas strong positive Zr (and Hf) anomalies are seen in the oxidized/doped experiments with very low REE mobility (Fig. 7a). In this case, the Sisson and Kelemen (2018) results are consistent with arc compositions, while Carter et al. (2015) has greater Zr/Zr^* than arcs (Fig. 7c).

None of the existing experiments provide a perfect fit to arc compositions. The absence of K_2O in Kessel (2005), the low K_2O and high, unconstrained f_{O2} of Carter et al. (2015), the high doping levels of the Klimm et al. (2008), the high K_2O of Luginbühl (2015) and the low f_{O2} of Sisson and Kelemen (2018) all apparently depart from conditions appropriate to most subducting slabs. The H_2O contents of most of these experiments are also higher than the water:rock ratios likely to be present during a given increment of flux melting. Though the individual experiments do not match the arc compositions directly, their systematic behavior suggests that ocean crust melts could indeed reproduce the range of observed compositions at moderate K_2O and trace element abundances, and intermediate f_{O2} . Under these conditions, a small amount of residual epidote could lead to high Sr/Sr^* without also producing high Zr/Zr^* .

We suggest that the best approach to quantify slab melting for Th and the REE is to interpolate between experimental end members. For elements controlled by epidote, we determined enrichment factors for a minimum bound defined by the 900 °C experiments of Klimm et al. (2008) and Carter et al. (2015), and the 800 °C experiment of Luginbühl (2015). A maximum bound was defined by the 900 °C experiment of Luginbühl and the 800 °C experiments of Sisson and Kelemen (Fig. 7a, Fig. S2). Using the Sr/Sr* and Zr/Zr* constraints as a guide, the compositions of 'hotter' and 'colder' slab melts were interpolated between these bounds, assuming the highest plausible elemental mobility in hot melts, and lower elemental mobility for the colder melts (Table 1). A visual depiction of this approach and more details of the enrichment factor calculations are available in the supplement.

For elements not strongly controlled by an accessory phase during melting (Pb, Cs, Rb, Ba, Sr), melt compositions were calculated as aggregated fractional melts using constant partition coefficients consistent with the ranges reported by Sisson and Kelemen (2018) and Carter et al. (2015), assuming melt fractions of 15% and 30% to be consistent with experiments containing moderate water contents for colder and hotter melts, respectively (Table 1). Nb and Ta abundances were calculated following the rutile partitioning model

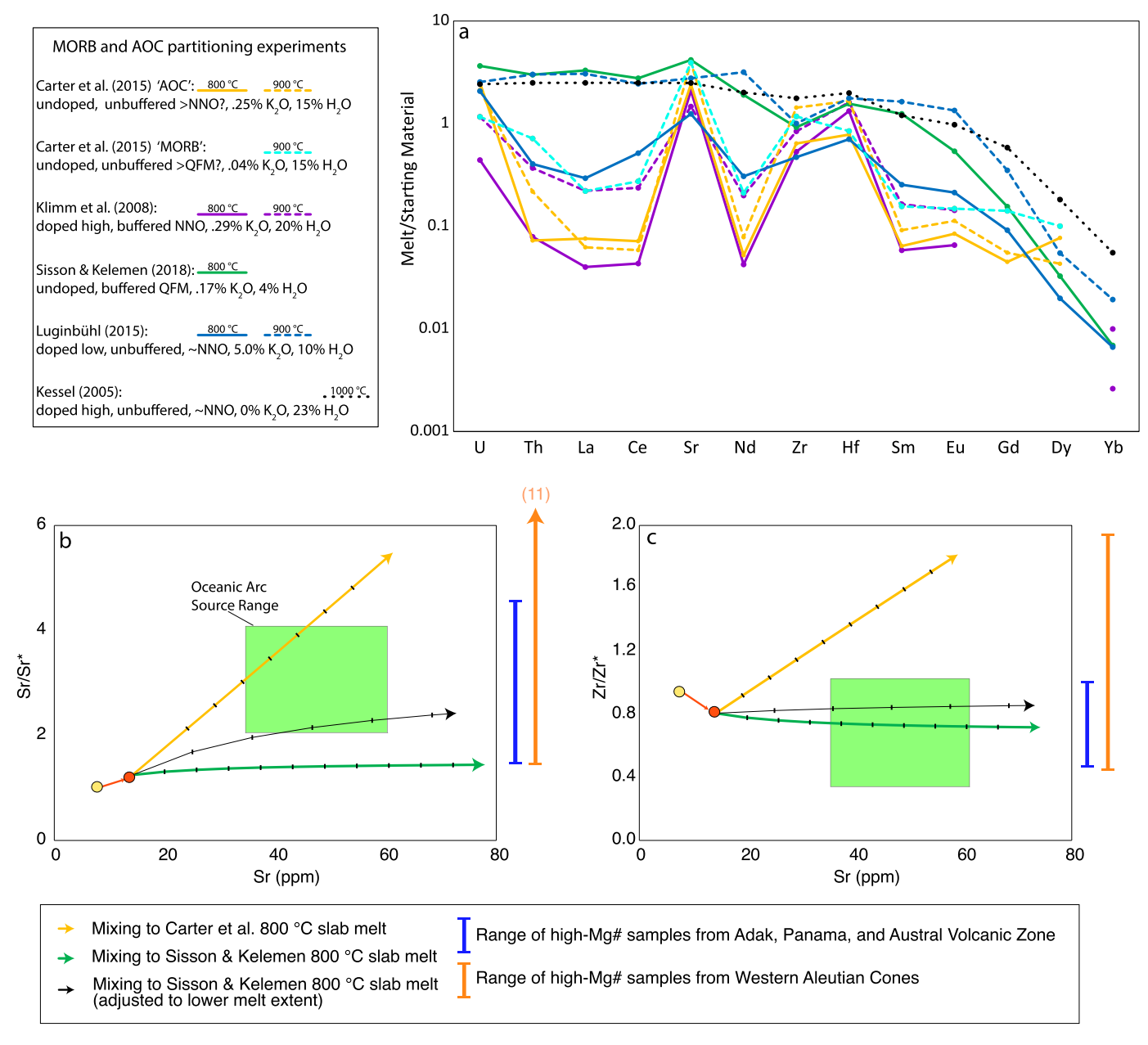


Fig. 7. (a) Experimental results of slab-melting analog experiments, with trace element abundances normalized to bulk starting compositions. Where necessary, the bulk compositions have been normalized to account for dilution by added water. (b) The green fields reflect the arc mantle source, and yellow/orange circles reflect a depleted mantle composition before/after the addition of sediment melt, as in Fig. 6. Abundances of elements that are incompatible during slab melting, such as Sr, should vary mostly as a function of the slab melting extent, while LREE are controlled by residual phases. Low extents of melting thus lead to high Sr/Sr*. Sisson and Kelemen (2018) suggest that the reduced melt fractions may be capable of producing arc compositions under these conditions. On panels b-c, the Sisson and Kelemen (2018) slab melt compositions are extrapolated to a melt fraction of 10%, at which point the mixing trajectory begins to intersect the range seen in arcs. While lower melt fractions could conceivably cause higher Sr/Sr*, this would require very low bulk water contents, and conflicts with the observation that high Sr/Sr* magmas are found in both the "hottest" and "coldest" slab environments. (c) To be consistent with the arc data, Nd and Sm mobilities during slab melting must be within the range of Zr and Hf, thus higher than the Carter et al. (2015) experiments. Sediment melt compositions are calculated using average D values from Table 1 and assuming 40% melt fraction, though the result is insensitive to melt fraction because the proportion of Sr that can be derived from sediment is limited by isotope mass balance, as in Fig. 6.

of Xiong et al. (2011), assuming 1.5% bulk TiO_2 and melt TiO_2 contents ranging from 0.2% in the colder melt to 0.5% in the hotter melt. In the natural AOC melting experiments of Carter et al. (2015), zircon is inferred in the lower-T experiments (with only 43 ppm Zr in the melt at 750 °C), but is exhausted between 850 and 900 °C. We assign 50 ppm Zr to the AOC melt for a typical colder slab melting scenario, and 110 ppm Zr for a somewhat hotter slab melt. Near the solidus, the Zr/Hf ratio in the melt is 35% lower than the bulk material, with negligible fractionation of Zr/Hf at higher temperatures as zircon breaks down. For our colder model slab melts, we therefore assign a Zr/Hf ratio that is 30% lower than

NMORB, while for the hotter slab melt we assign a Zr/Hf ratio that is equal to NMORB. Fig. 8 demonstrates the resulting range of model AOC melt trace element compositions.

3.2. Calculation of sediment melts

While AOC melts dominate the Sr budget of volcanic arcs, it is clear that most of the other enrichments in highly incompatible elements are largely derived from subducting sediment (e.g., Figs. 1–2). In contrast to the undoped ocean crust melting experiments, the high P_2O_5 and REE abundances in natural sediments

Table 1 AOC and sediment melting partition coefficients.

	AOC Melt Model Compositions					Sediment D's	
	'very cold'	'colder'	'moderate'	'hotter'		hotter	colder
melt fraction	0.1	0.15	0.2	0.3			
TiO ₂ ^d	2000	2000	3000	5000			
Rb ^a	16.2	11.8	9.1	6.1	Rb	0.7	0.7
Sr ^a	834	685	571	415	Sr	0.25	0.25
Zr ^ℂ	50	50	62	111	Zr	1.8	4
Nb ^d	0.58	0.53	0.73	1.07	Nb	2	7.5
Cs ^a	0.24	0.24	0.12	0.08	Cs	0.1	0.1
Ba ^a	172	126	97	65	Ba	0.4	0.4
La ^b	1.51	3.19	3.71	4.78	La	0.83	2.3
Ce ^b	4.47	9.16	10.57	13.48	Ce	0.9	2.5
Nd ^b	3.84	7.42	8.46	10.58	Nd	1.6	3.5
Sm ^b	1.04	1.80	2.01	2.42	Sm	2.2	4
Eu ^b	0.26	0.43	0.47	0.56	Eu	2.8	4.4
\mathbf{Gd}^{b}	0.73	0.92	0.96	1.04	Gd	4	7
$\mathbf{D}\mathbf{y}^{\mathrm{b}}$	0.30	0.34	0.35	0.37	Dy	9	14
Er ^b	0.09	0.10	0.10	0.10	Er	16	20
Yb ^b	0.05	0.05	0.06	0.06	Yb	50	60
Lu ^b	0.01	0.01	0.01	0.01	Lu	75	90
Hf ^c	2.19	2.19	0.00	2.68	Hf	1.2	2.6
Ta ^d	0.02	0.04	0.04	0.07	Ta	1.8	7.5
Pb ^a	2.57	2.25	1.97	1.54	Pb	0.5	0.7
Th ^b	0.20	0.20	0.37	0.44	Th	0.6	1.4
U ^b	0.33	0.33	0.33	0.33	U	0.4	0.7

 $^{^{}a}$ Values were calculated using constant partition coefficients (DRb=0.05, DSr=0.1, DCs=0.01, DBa=0.05, DPb=0.15).

^d TiO₂ abundances following Carter et al. (2015). Nb and Ta D values based on residual rutile proportion, given 1.5 wt.% bulk TiO₂. Nb and Ta D values based the systematics described by Xiong et al. (2011, see their Fig. 11). DNb decreases from 400 to 200. DNb/DTa is 0.5 for the 'very cold melt', 0.9 for the intermediate melts, and 1 for the 'hotter' melt.

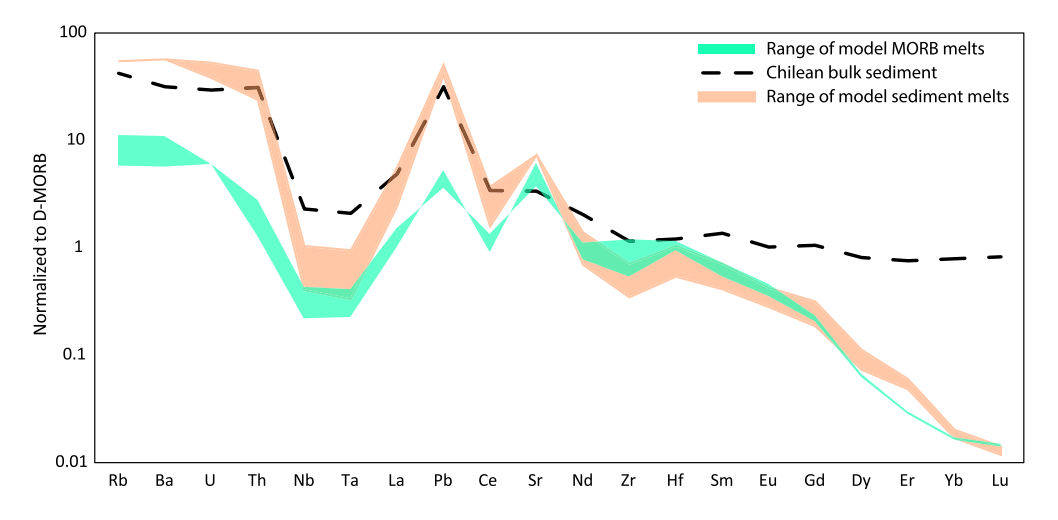


Fig. 8. Examples of calculated slab components normalized to MORB, as described in the text and available in Table 1. The range of MORB melt compositions for melt fractions from 15-30% are plotted in green (the 'very cold' AOC melt of Table 1 is inferred to be relevant only in unusual settings and is not plotted). Note that this is strictly a "MORB" melt composition, not adjusted for the potential enrichment of Rb, U, or Ba during seafloor alteration. U, Pb, Cs, Rb, Ba, and Sr are assumed to behave incompatibly with constant D values (Table 1). Elemental abundances in the melt for these elements are calculated using the aggregate fractional melting equation $Cl=(Co/F)^*(1-(1-F)^*(1/D))$. Strontium, with a D value of 0.1, then varies from 415 to 685 ppm in the melt. The REE abundances are extrapolated based on 'enrichment factors' relative to bulk abundances from the experimental data in Fig. 7 at 800 and 900 °C (see online supplement). Nb and Ta partitioning are calculated following Xiong et al. (2011). Zr and Hf are controlled by a combination of garnet and zircon (see text). Sediment melt compositions are calculated similarly to the MORB melt, though REE values are calculated from T-dependent D values (Table 1). An example of sediment melt compositions derived from the bulk sediment composition of DSDP 1232 (Turner et al., 2017), sampled offshore of Southern Chile (black dotted line) are plotted in light brown.

may stabilize monazite during melting (Hermann and Rubatto, 2009; Skora and Blundy, 2010) in which case the LREE+Th serve as essential structural constituents (ESCs). Hanson and Langmuir (1978) define an ESC as "an element which completely fills one site in a mineral and for which there is very little solid solution." In the case of monazite, the LREE can be considered collectively as

an ESC as long as their total abundances are well in excess of Th (Skora and Blundy, 2010). Under these conditions, the concentration of an ESC in the melt may be independent of the proportion of that mineral in the system and vary only with melt composition and temperature. Adding more Zr to a system that is saturated in zircon, for example, will not impact the Zr concentration of the

^b Element abundances interpolated from experimental enrichment factors, see text and online supplement for details.

c See text.

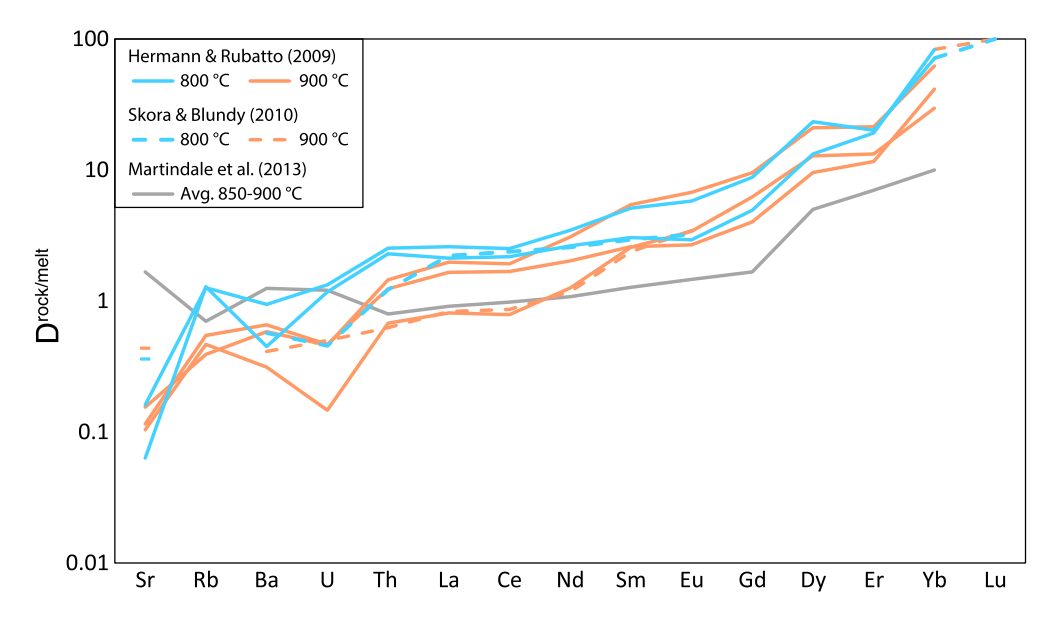


Fig. 9. Sediment melting bulk partition coefficients, calculated via mass balance from bulk starting material compositions and reported melt extents and melt compositions from the experiments of Hermann and Rubatto (2009) and Skora and Blundy (2010), and taken directly from Martindale et al. (2013). Note that despite substantially different bulk compositions, the experiments of Hermann and Rubatto (2009) and Skora and Blundy (2010) provide similar bulk D values, with a clear temperature dependence for the LREE. These indicate that a LREE-based slab thermometer will need to include information about bulk sediment compositions. The experiments of Martindale et al. (2013), in contrast, used an enriched volcaniclastic sediment as the starting composition, with differing results for several elements (see text for discussion).

melt, it will just create more zircon. Plank et al. (2009) proposed that the LREE abundances during sediment melting might behave in a similar way, in which case the LREE abundances in a sediment melt could be used as a slab thermometer.

The studies of Skora and Blundy (2010, 2012), however, show that REE and Th abundances also change with bulk composition at a single temperature, which implies that these elements cannot be used as a reliable slab thermometer. This probably occurs because the LREE and phosphorus species become disassociated in the melt (Skora and Blundy, 2012). At low and moderate phosphorus concentrations, the addition of LREE to a monazite-saturated system will therefore not lead to a directly proportional increase in modal monazite, and the melt's LREE abundances will increase. This result is also apparent by comparing the 800 °C experimental melts (~7% Bulk H₂O) of Hermann and Rubatto (2009) with those of Skora and Blundy (2010). These experimental melts differ in Ce concentration by a factor of two (33 vs 66 ppm), which is proportional to their bulk experimental Ce abundances (68 vs 156 ppm), as would be expected if their melt abundances were controlled by bulk composition in addition to temperature.

A comprehensive treatment of LREE and Th partitioning during sediment melting would therefore need to include information on the bulk sediment's LREE and phosphorus concentrations as well as an accurate model of apatite saturation, which also depends on calcium (Skora and Blundy, 2012). These considerations will be especially important for studies of uranium-series systematics (e.g., Avanzinelli et al., 2012) because the relative proportions of residual apatite vs monazite can control the partitioning of U and Th, as seen from the large differences in slope between U and Th on Fig. 9.

In the absence of experiments under suitable conditions for all of the diverse sediments subducting beneath arcs, modeling melts of sediment remains a challenge. At present, attempts at this endeavor still benefit from some general observations of the available data. Fig. 9 shows calculated solid/melt partition coefficients for the experiments of both Hermann and Rubatto (2009) and Skora and Blundy (2010). Despite substantially different bulk compositions, the Ds for most elements vary by only a factor of 2 or 3, and in the case of the LREE, the variation within a given

temperature bracket is even more limited. This suggests that an empirical parameterization of temperature-dependent bulk partition coefficients based on available experiments can be used to model sediment melting as a function of bulk sediment composition and melt extent. Table 1 provides a set of 'colder' and 'hotter' sediment melting partition coefficients that can be used to model trace element distribution during slab melting. To calculate Nb and Ta abundances in the melts requires bulk TiO2 abundances and melting extents, which can be accomplished using the rutile model of Xiong et al. (2011). Zr and Hf bulk D's for 'hotter' and 'colder' slabs are based on Hermann and Rubatto (2009). An example application of this sediment melting model to the southern Chilean subduction zone is shown in Fig. 8. The relative differences between the sediment source and its partial melt may be similar for different subduction zones, but the details of the pattern and its abundances will depend critically on the sediment composition.

This approach to sediment melting is not likely to be successful for the entire range of sediment compositions, however. For example, melting experiments (Martindale et al., 2013) on the OIB-like volcaniclastic sediments subducting beneath the Marianas (Fig. 9) have significantly lower bulk D values for the HREE (due to a lower proportion of residual garnet) and an unusually high D value for Sr (the host for which was not identified). While these volcaniclastic sediment melting partition coefficients have been used to model elemental mobility in the Cascades (Mullen et al., 2017), they are more likely only applicable to enriched volcaniclastic compositions and will produce erroneous results elsewhere. Results for carbonate-rich compositions also differ (Skora et al., 2015; Avanzinelli et al., 2018). Therefore, while the approach we propose may be useful for most subducting sediments, there is a clear need for continued experimental work on sediment melting of diverse compositions.

4. Implications for slab thermometers

Sediment melt H_2O concentrations have also been suggested to be controlled primarily by slab temperature, with lower H_2O contents at higher temperatures (Hermann and Spandler, 2008). If melting of the dehydrated upper slab occurs during incremental

dehydration of deeper slab lithologies, however, then the bulk H₂O contents at any given moment during melting should always be low. Analog experiments with low bulk H₂O (Mann and Schmidt, 2015) appear to produce melts that also have lower H₂O in some cases. In addition, it has been suggested that early slab dehydration may stabilize chlorite above the slab surface, which would later dehydrate near the arc front (Grove et al., 2012, Fig. 3b). If H₂O lost from the slab in between the coupling depth and the onset of slab melting is consumed by chlorite production above the slab, it can be anticipated that chloritized peridotite may occupy a layer that is over 1 km thick (Figs. 3c-e). The thermal models indicate that this chlorite would become destabilized across the same depth range that melting occurs in the underlying slab (Fig. 3b-e), and thus would presumably become incorporated into the slab melt, further decoupling the melt H₂O concentration from the slab temperature.

Finally, while results from the LREE/H2O slab thermometer initially appeared consistent with numerical modeling results (Cooper et al., 2012), there are important sources of uncertainty associated with these models. For example, shear heating on the surface of the slab is probably an important process (England, 2018), and models that incorporate shear heating predict a smaller range in slab-surface temperatures than are suggested by the H₂O/Ce thermometer (van Keken et al., 2018). Incorporating the latent heat of melting would exacerbate this discrepancy. Given a heat capacity of 1484 J/kg K and a specific heat of fusion of 570 kJ/kg (Lesher and Spera, 2015), for example, extraction of 30% melt from an eclogite should cool the rock by \sim 115 °C. Additional melting should therefore cool down the hottest slabs and further limit the global range of sub-arc slab temperatures. While the importance of slab temperature variations to arc geochemistry remains an open question, it is clear that recent experimental evidence and a variety of other concerns still complicate the reliability of a conceptually simple slab thermometer.

5. On adakites

If melting of both ocean crust and sediment are required to account for the compositions of all arc-front stratovolcano compositions, then a more nuanced interpretation is needed for 'adakites' arc rocks which have up to ~2000ppm Sr, and often below 1 ppm Yb. Adakites predominantly erupt near subducting oceanic ridges and where subduction is oblique or very slow, such as in Panama (Gazel et al., 2015), the Western Aleutians (Kelemen et al., 2003a, Yogodzinski et al., 2017), and the Austral Volcanic Zone of Chile (Stern and Kilian, 1996). These conditions lead to hotter-thanaverage slabs with colder-than-average overlying mantle. Adakites may then be a consequence of a larger proportion of slab melt and a lesser contribution from wedge melting. Because the HREE abundances in adakites are diluted by about a factor of two relative to typical arc-front stratovolcanoes, one could infer that their 'mantle source' has been diluted at least 50% by a slab melt that is essentially devoid of HREE, as compared to the 5-7% slab melt required to account for the Sr budgets of normal arc- front volcanics (Fig. 6). At such high proportions of slab melt, however, the flux dominates the source composition and the process is more aptly described as 'melt-rock reaction' (Kelemen et al., 2003a), especially since colder mantle wedge temperatures may lead to decreasing rather than increasing melt abundance as the slab melts ascend. The conditions of slab melting in these tectonic environments may also differ from more typical arc segments. Very hot slabs probably dehydrate more at shallower depths, leading to lower extents of slab melting at great depths beneath the arc.

Despite these caveats, high-Mg# rocks from most adakite locales appear consistent with the model of slab melting presented in Fig. 8, because most adakites have Sr/Sr* and Zr/Zr* ranges that overlap with more typical arc volcanics (Fig. 7b-c). In con-

trast, the Western Aleutian Cones (Yogodzinski et al., 2017) span a much larger compositional range, with Sr/Sr* as high as 11, and Zr/Zr* as high as 2. If the trace element abundances of these rocks reflect pristine slab melt compositions, then it appears that the conditions of melting beneath the Western Aleutian Cones must differ. It should be cautioned, however, that the felsic melt compositions found in many of these locales will not fractionate mafic minerals, in which case the Mg# may not serve as an appropriate index of crystal fractionation, and the high Mg# seen in some samples may not necessarily ensure that they are undifferentiated. Assuming these compositions are in fact representative of primary mantle melts, the differences between the Western Aleutian cones and other adakites may arise due to either lower extents of slab melting (which could result from more extensive early slab dehydration) or else higher oxygen fugacity during melting.

6. Conclusions

The literature on convergent margin volcanism has not come to a consensus on the nature of the flux from the down-going slab. While it is generally agreed that sediments must melt, there has been widespread disagreement regarding whether the component from altered ocean crust is a fluid or a melt. We have presented several lines of evidence towards resolution of this controversy, all of which support ubiquitous melting of igneous ocean crust. The wealth of experimental data shows that the mobilities of many elements in sub-solidus fluids, most notably Sr, are insufficient to satisfy mass-balance at arcs. In contrast, slab melts readily transport sufficient Sr, and appear to be the sole means to account for the universally raised Sr/Nd of arc volcanics. Melting of the crust is also consistent with recent thermal models. An evaluation of the spectrum of recent experimental results permits calculation of the compositions of the melts from both igneous ocean crust and sediment. These compositions can then provide the necessary inputs to constrain both regional and global models of arc volcanism.

CRediT authorship contribution statement

Stephen J. Turner: Conceptualization, Data curation, Quantitative analysis, Visualization, Writing - original draft, **Charles H. Langmuir:** Conceptualization, Writing - original draft.

Declaration of competing interest

The authors declare that they have no known competing financial interests or personal relationships that could have appeared to influence the work reported in this paper.

Acknowledgements

The authors thank Peter van Keken, who provided temperature grids from published thermal models and two anonymous reviewers for constructive comments which improved this manuscript. This work was supported by NSF grant EAR-1939080 to the University of Massachusetts Amherst and NSF grants OCE-1634421 and EAR-0948511 to Harvard University.

Appendix A. Supplementary material

Supplementary material related to this article can be found online at https://doi.org/10.1016/j.epsl.2022.117424.

References

Aiuppa, A., Fischer, T.P., Plank, T., Robidoux, P., Di Napoli, R., 2017. Along-arc, interarc and arc-to-arc variations in volcanic gas CO2/ST ratios reveal dual source of carbon in arc volcanism. Earth-Sci. Rev. 168, 24–47.

- Avanzinelli, R., Casalini, M., Elliott, T., Conticelli, S., 2018. Carbon fluxes from subducted carbonates revealed by uranium excess at Mount Vesuvius, Italy. Geology 46, 259–262.
- Avanzinelli, R., Prytulak, J., Skora, S., Heumann, A., Koetsier, G., Elliott, T., 2012. Combined ²³⁸U–²³⁰Th and ²³⁵U–²³¹Pa constraints on the transport of slab-derived material beneath the Mariana Islands. Geochim. Cosmochim. Acta 92, 308–328.
- Bach, W., Peucker-Ehrenbrink, B., Hart, S.R., Blusztajn, J.S., 2003. Geochemistry of hydrothermally altered oceanic crust: DSDP/ODP Hole 504B-implications for seawater-crust exchange budgets and Sr-and Pb-isotopic evolution of the mantle. Geochem. Geophys. Geosyst. 4.
- Bekaert, D., Turner, S., Broadley, M., Barnes, J., Halldórsson, S., Labidi, J., Wade, J., Walowski, K., Barry, P., 2021. Subduction-driven volatile recycling: a global mass balance. Annu. Rev. Earth Planet. Sci. 49.
- Bezard, R., Davidson, J.P., Turner, S., Macpherson, C.G., Lindsay, J.M., Boyce, A.J., 2014.

 Assimilation of sediments embedded in the oceanic arc crust: Myth or reality?

 Earth Planet. Sci. Lett. 395. 51–60.
- Borchert, M., Wilke, M., Schmidt, C., Rickers, K., 2010. Rb and Sr partitioning between haplogranitic melts and aqueous solutions. Geochim. Cosmochim. Acta 74, 1057–1076.
- Brenan, J., Shaw, H., Ryerson, F., Phinney, D., 1995. Mineral-aqueous fluid partitioning of trace elements at 900°C and 2.0 GPa: constraints on the trace element chemistry of mantle and deep crustal fluids. Geochim. Cosmochim. Acta 59, 3331–3350.
- Brounce, M., Kelley, K., Cottrell, E., 2014. Variations in Fe³⁺/ \sum Fe of Mariana Arc basalts and mantle wedge f O₂. J. Petrol. 55, 2513–2536.
- Carter, L.B., Skora, S., Blundy, J., De Hoog, J., Elliott, T., 2015. An experimental study of trace element fluxes from subducted oceanic crust. J. Petrol. 56, 1585–1606.
- Castillo, P., 2021. Arc magmatism and porphyry-type ore deposition are primarily controlled by chlorine from seawater. Chem. Geol., 120683.
- Class, C., Miller, D.M., Goldstein, S.L., Langmuir, C.H., 2000. Distinguishing melt and fluid subduction components in Umnak Volcanics, Aleutian Arc. Geochem. Geophys. Geosyst. 1.
- Cooper, L.B., Ruscitto, D.M., Plank, T., Wallace, P.J., Syracuse, E.M., Manning, C.E., 2012. Global variations in H₂O/Ce: 1. Slab surface temperatures beneath volcanic arcs. Geochem. Geophys. Geosyst. 13.
- Davidson, J.P., Harmon, R.S., 1989. Oxygen isotope constraints on the petrogenesis of volcanic arc magmas from Martinique, Lesser Antilles. Earth Planet. Sci. Lett. 95, 255–270.
- Defant, M.J., Drummond, M.S., 1990. Derivation of some modern arc magmas by melting of Young subducted lithosphere. Nature 347, 662–665.
- Dimalanta, C., Taira, A., Yumul Jr, G., Tokuyama, H., Mochizuki, K., 2002. New rates of western Pacific island arc magmatism from seismic and gravity data. Earth Planet. Sci. Lett. 202, 105–115.
- Dixon, J.E., Bindeman, I., Kingsley, R.H., Simons, K., Le Roux, P., Hajewski, T., Swart, P., Langmuir, C., Ryan, J., Walowski, K., 2017. Light stable isotopic compositions of enriched mantle sources: resolving the dehydration paradox. Geochem. Geophys. Geosyst. 18, 3801–3839.
- Duggen, S., Portnyagin, M., Baker, J., Ulfbeck, D., Hoernle, K., Garbe-Schönberg, D., Grassineau, N., 2007. Drastic shift in lava geochemistry in the volcanic-front to rear-arc region of the Southern Kamchatkan subduction zone: evidence for the transition from slab surface dehydration to sediment melting. Geochim. Cosmochim. Acta 71, 452–480.
- Durkin, K., Castillo, P.R., Straub, S.M., Abe, N., Tamura, Y., Yan, Q., 2020. An origin of the along-arc compositional variation in the Izu-Bonin arc system. Geosci. Front. 11, 1621–1634.
- Ellam, R., Hawkesworth, C., 1988. Elemental and isotopic variations in subduction related basalts: evidence for a three component model. Contrib. Mineral. Petrol. 98, 72–80.
- Elliott, T., 2003. Tracers of the Slab. Geophysical Monograph-American Geophysical Union, vol. 138, pp. 23–46.
- Elliott, T., Plank, T., Zindler, A., White, W., Bourdon, B., 1997. Element transport from slab to volcanic front at the Mariana arc. J. Geophys. Res., Solid Earth 102, 14991–15019.
- England, P., 2018. On shear stresses, temperatures, and the maximum magnitudes of earthquakes at convergent plate boundaries. J. Geophys. Res., Solid Earth 123, 7165–7202.
- Frei, D., Liebscher, A., Wittenberg, A., Shaw, C.S., 2003. Crystal chemical controls on rare Earth element partitioning between epidote-group minerals and melts: an experimental and theoretical study. Contrib. Mineral. Petrol. 146, 192–204.
- Freymuth, H., Ivko, B., Gill, J.B., Tamura, Y., Elliott, T., 2016. Thorium isotope evidence for melting of the mafic oceanic crust beneath the izu arc. Geochim. Cosmochim. Acta 186, 49–70.
- Fumagalli, P., Poli, S., 2005. Experimentally determined phase relations in hydrous peridotites to 6.5 GPa and their consequences on the dynamics of subduction zones. J. Petrol. 46, 555–578.
- Furukawa, Y., 1993. Depth of the decoupling plate interface and thermal structure under arcs. J. Geophys. Res., Solid Earth 98, 20005–20013.
- Gale, A., Dalton, C.A., Langmuir, C.H., Su, Y., Schilling, J.G., 2013. The mean composition of ocean ridge basalts. Geochem. Geophys. Geosyst. 14, 489–518.

- Gazel, E., Hayes, J.L., Hoernle, K., Kelemen, P., Everson, E., Holbrook, W.S., Hauff, F., van den Bogaard, P., Vance, E.A., Chu, S., 2015. Continental crust generated in oceanic arcs. Nat. Geosci. 8, 321–327.
- Gómez-Tuena, A., Langmuir, C.H., Goldstein, S.L., Straub, S.M., Ortega-Gutiérrez, F., 2007. Geochemical evidence for slab melting in the Trans-Mexican Volcanic Belt. J. Petrol. 48, 537–562.
- Grove, T.L., Till, C.B., Krawczynski, M.J., 2012. The role of H_2O in subduction zone magmatism. Annu. Rev. Earth Planet. Sci. 40, 413–439.
- Hacker, B.R., 2008. H2O subduction beyond arcs. Geochem. Geophys. Geosyst. 9.
- Handley, H.K., Blichert-Toft, J., Gertisser, R., Macpherson, C.G., Turner, S.P., Zaennudin, A., Abdurrachman, M., 2014. Insights from Pb and O isotopes into along-arc variations in subduction inputs and crustal assimilation for volcanic rocks in Java, Sunda arc, Indonesia. Geochim. Cosmochim. Acta 139, 205–226.
- Hanson, G.N., Langmuir, C.H., 1978. Modelling of major elements in mantlemelt systems using trace element approaches. Geochim. Cosmochim. Acta 42, 725–741.
- Hermann, J., Rubatto, D., 2009. Accessory phase control on the trace element signature of sediment melts in subduction zones. Chem. Geol. 265, 512–526.
- Hermann, J., Spandler, C.J., 2008. Sediment melts at sub-arc depths: an experimental study. J. Petrol. 49, 717–740.
- Jicha, B.R., Jagoutz, O., 2015. Magma production rates for intraoceanic arcs. Elements 11, 105–111.
- Johnson, M.C., Plank, T., 2000. Dehydration and melting experiments constrain the fate of subducted sediments. Geochem. Geophys. Geosyst. 1.
- Kawamoto, T., Mibe, K., Bureau, H., Reguer, S., Mocuta, C., Kubsky, S., Thiaudière, D., Ono, S., Kogiso, T., 2014. Large-ion lithophile elements delivered by saline fluids to the sub-arc mantle. Earth Planets Space 66, 1–11.
- Kelemen, P., Yogodzinski, G., Scholl, D., 2003a. Along-strike variation in lavas of the Aleutian island arc: Implications for the genesis of high Mg# andesite and the continental crust. Inside the subduction factory. In: Inside the Subduction Factory, Geophysical Monograph, vol. 138, pp. 223–276.
- Kelemen, P.B., Hanghøj, K., Greene, A., 2003b. One View of the Geochemistry of Subduction-Related Magmatic Arcs, with an Emphasis on Primitive Andesite and Lower Crust. Treatise on Geochemistry, vol. 3, p. 659.
- Kelemen, P.B., Rilling, J.L., Parmentier, E., Mehl, L., Hacker, B.R., 2003c. Thermal Structure Due to Solid-State Flow in the Mantle Wedge Beneath Arcs. Geophysical Monograph-American Geophysical Union, vol. 138, pp. 293–311.
- Keppler, H., 1996. Constraints from partitioning experiments on the composition of subduction-zone fluids. Nature 380, 237–240.
- Kessel, R., Schmidt, M.W., Ulmer, P., Pettke, T., 2005. Trace element signature of subduction-zone fluids, melts and supercritical liquids at 120–180 km depth. Nature 437, 724–727.
- Klaver, M., Lewis, J., Parkinson, I.J., Elburg, M.A., Vroon, P.Z., Kelley, K.A., Elliott, T., 2020. Sr isotopes in arcs revisited: tracking slab dehydration using $\delta^{88/86}$ Sr and 87 Sr/ 86 Sr systematics of arc lavas. Geochim. Cosmochim. Acta 288, 101–119.
- Klimm, K., Blundy, J.D., Green, T.H., 2008. Trace element partitioning and accessory phase saturation during H2O-saturated melting of basalt with implications for subduction zone chemical fluxes. J. Petrol. 49, 523–553.
- Labanieh, S., Chauvel, C., Germa, A., Quidelleur, X., 2012. Martinique: a clear case for sediment melting and slab dehydration as a function of distance to the trench. J. Petrol. 53, 2441–2464.
- Lesher, C.E., Spera, F.J., 2015. Thermodynamic and transport properties of silicate melts and magma. In: The Encyclopedia of Volcanoes. Elsevier, pp. 113–141.
- Li, H., Hermann, J., 2015. Apatite as an indicator of fluid salinity: an experimental study of chlorine and fluorine partitioning in subducted sediments. Geochim. Cosmochim. Acta 166, 267–297.
- Liu, J., Bohlen, S., Ernst, W., 1996. Stability of hydrous phases in subducting oceanic crust. Earth Planet. Sci. Lett. 143, 161–171.
- Luginbühl, S.M., 2015. Phase Relations, Compositions and Trace Element Partitioning of Solid and Mobile Phases in the Hydrous MORB System at 2-3 GPa. ETH, Zurich
- Mann, U., Schmidt, M.W., 2015. Melting of pelitic sediments at subarc depths: 1. Flux vs. fluid-absent melting and a parameterization of melt productivity. Chem. Geol. 404, 150–167.
- Manning, C.E., 2004. The chemistry of subduction-zone fluids. Earth Planet. Sci. Lett. 223, 1–16.
- Martindale, M., Skora, S., Pickles, J., Elliott, T., Blundy, J., Avanzinelli, R., 2013. High pressure phase relations of subducted volcaniclastic sediments from the West Pacific and their implications for the geochemistry of Mariana arc magmas. Chem. Geol. 342, 94–109.
- Miller, D.M., Goldstein, S.L., Langmuir, C.H., 1994. Cerium/lead and lead isotope ratios in arc magmas and the enrichment of lead in the continents. Nature 368, 514–520.
- Mullen, E., Weis, D., Marsh, N., Martindale, M., 2017. Primitive arc magma diversity: new geochemical insights in the Cascade Arc. Chem. Geol. 448, 43–70.
- Ni, H., Zhang, L., Xiong, X., Mao, Z., Wang, J., 2017. Supercritical fluids at subduction zones: evidence, formation condition, and physicochemical properties. Earth-Sci. Rev. 167, 62–71.
- Plank, T., 2005. Constraints from thorium/lanthanum on sediment recycling at subduction zones and the evolution of the continents. J. Petrol. 46, 921–944.

- Plank, T., 2013. The Chemical Composition of Subducting Sediments. The Crust, Treatise on Geochemistry. vol. 4.
- Plank, T., 2014. 4.17 The Chemical Composition of Subducting Sediments. In: Holland, Heinrich D., Turekian, Karl K. (Eds.), Treatise on Geochemistry (Second Edition). Elsevier. ISBN 9780080983004, pp. 607–629.
- Plank, T., Langmuir, C.H., 1993. Tracing trace elements from sediment input to volcanic output at subduction zones. Nature 362, 739–743.
- Plank, T., Cooper, L.B., Manning, C.E., 2009. Emerging geothermometers for estimating slab surface temperatures. Nat. Geosci. 2, 611–615.
- Plank, T., Kelley, K.A., Zimmer, M.M., Hauri, E.H., Wallace, P.J., 2013. Why do mafic arc magmas contain \sim 4 wt% water on average? Earth Planet. Sci. Lett. 364, 168–179
- Poli, S., Schmidt, M.W., 2002. Petrology of subducted slabs. Annu. Rev. Earth Planet. Sci. 30, 207–235.
- Rustioni, G., Audétat, A., Keppler, H., 2019. Experimental evidence for fluid-induced melting in subduction zones. Geochem. Perspect. Lett. 11, 49–54.
- Schmidt, M.W., Jagoutz, O., 2017. The global systematics of primitive arc melts. Geochem. Geophys. Geosyst. 18, 2817–2854.
- Schmidt, M.W., Poli, S., 1998. Experimentally based water budgets for dehydrating slabs and consequences for arc magma generation. Earth Planet. Sci. Lett. 163, 361–379.
- Schmidt, M.W., Vielzeuf, D., Auzanneau, E., 2004. Melting and dissolution of subducting crust at high pressures: the key role of white mica. Earth Planet. Sci. Lett. 228, 65–84.
- Singer, B.S., Jicha, B.R., Leeman, W.P., Rogers, N.W., Thirlwall, M.F., Ryan, J., Nicolaysen, K.E., 2007. Along-strike trace element and isotopic variation in Aleutian island arc basalt: subduction melts sediments and dehydrates serpentine. J. Geophys. Res., Solid Earth 112.
- Sisson, T., Kelemen, P., 2018. Near-solidus melts of MORB+ 4 wt.% H₂O at 0.8-2.8 GPa applied to issues of subduction magmatism and continent formation. Contrib. Mineral. Petrol. 173. 1-23.
- Skora, S., Blundy, J., 2010. High-pressure hydrous phase relations of radiolarian clay and implications for the involvement of subducted sediment in arc magmatism. J. Petrol. 51, 2211–2243.
- Skora, S., Blundy, J., 2012. Monazite solubility in hydrous silicic melts at high pressure conditions relevant to subduction zone metamorphism. Earth Planet. Sci. Lett. 321, 104–114.
- Skora, S., Blundy, J.D., Brooker, R.A., Green, E.C., de Hoog, J., Connolly, J.A., 2015. Hydrous phase relations and trace element partitioning behaviour in calcareous sediments at subduction-zone conditions. J. Petrol. 56, 953–980.
- Spandler, C., Mavrogenes, J., Hermann, J., 2007. Experimental constraints on element mobility from subducted sediments using high-P synthetic fluid/melt inclusions. Chem. Geol. 239, 228–249.
- Spandler, C., Pirard, C., 2013. Element recycling from subducting slabs to arc crust: a review. Lithos 170, 208–223.

- Stalder, R., Foley, S., Brey, G., Horn, I., 1998. Mineral-aqueous fluid partitioning of trace elements at 900–1200 C and 3.0–5.7 GPa: new experimental data for garnet, clinopyroxene, and rutile, and implications for mantle metasomatism. Geochim. Cosmochim. Acta 62, 1781–1801.
- Staudigel, H., Davies, G., Hart, S.R., Marchant, K., Smith, B.M., 1995. Large scale isotopic Sr, Nd and O isotopic anatomy of altered oceanic crust: DSDP/ODP sites 417/418. Earth Planet. Sci. Lett. 130, 169–185.
- Stern, C.R., Kilian, R., 1996. Role of the subducted slab, mantle wedge and continental crust in the generation of adakites from the Andean Austral Volcanic Zone. Contrib. Mineral. Petrol. 123, 263–281.
- Stolper, E., Newman, S., 1994. The role of water in the petrogenesis of Mariana trough magmas. Earth Planet. Sci. Lett. 121, 293–325.
- Turner, S.J., Langmuir, C.H., 2015. The global chemical systematics of arc front stratovolcanoes: evaluating the role of crustal processes. Earth Planet. Sci. Lett. 422, 182–193.
- Turner, S.J., Langmuir, C.H., 2022. An evaluation of five models of arc volcanism. J. Petrol. https://doi.org/10.1093/petrology/egac010.
- Turner, S.J., Langmuir, C.H., Dungan, M.A., Escrig, S., 2017. The importance of mantle wedge heterogeneity to subduction zone magmatism and the origin of EM1. Earth Planet. Sci. Lett. 472, 216–228.
- Turner, S.J., Langmuir, C.H., Katz, R.F., Dungan, M.A., Escrig, S., 2016. Parental arc magma compositions dominantly controlled by mantle-wedge thermal structure. Nat. Geosci. 9, 772–776.
- Van Keken, P.E., Kiefer, B., Peacock, S.M., 2002. High-resolution models of subduction zones: implications for mineral dehydration reactions and the transport of water into the deep mantle. Geochem. Geophys. Geosyst. 3. 1 of 20-20 of 20.
- van Keken, P.E., Wada, I., Abers, G.A., Hacker, B.R., Wang, K., 2018. Mafic highpressure rocks are preferentially exhumed from warm subduction settings. Geochem. Geophys. Geosyst. 19, 2934–2961.
- Wada, I., Behn, M.D., Shaw, A.M., 2012. Effects of heterogeneous hydration in the incoming plate, slab rehydration, and mantle wedge hydration on slab-derived H2O flux in subduction zones. Earth Planet. Sci. Lett. 353, 60–71.
- Wada, I., Wang, K., 2009. Common depth of slab-mantle decoupling: reconciling diversity and uniformity of subduction zones. Geochem. Geophys. Geosyst, 10.
- Wei, C., Duan, Z., 2019. Phase Relations in Metabasic Rocks: Constraints from the Results of Experiments, Phase Modelling and ACF Analysis. Special Publications, vol. 474. Geological Society, London, pp. 25–45.
- Xiong, X., Keppler, H., Audétat, A., Ni, H., Sun, W., Li, Y., 2011. Partitioning of Nb and Ta between rutile and felsic melt and the fractionation of Nb/Ta during partial melting of hydrous metabasalt. Geochim. Cosmochim. Acta 75, 1673–1692.
- Yogodzinski, G.M., Kelemen, P.B., Hoernle, K., Brown, S.T., Bindeman, I., Vervoort, J.D., Sims, K.W., Portnyagin, M., Werner, R., 2017. Sr and O isotopes in western Aleutian seafloor lavas: Implications for the source of fluids and trace element character of arc volcanic rocks. Earth Planet. Sci. Lett. 475, 169–180.